Thin Solid Films 518 (2010) 3228–3233

Contents lists available at ScienceDirect

Thin Solid Films

journal homepage: www.elsevier.com/locate/tsf

Deposition of the fractal-like gold particles onto electrospun polymethylmethacrylate fibrous mats and their application in surface-enhanced Raman scattering

Bin Guo, Gaoyi Han *, Miaoyu Li, Shizhen Zhao

Institute of Molecular Science, Key Laboratory of Chemical Biology and Molecular Engineering of Education Ministry, Shanxi University, Taiyuan 030006, PR China

ARTICLE INFO

Article history:
Received 19 November 2008
Received in revised form 14 October 2009
Accepted 27 October 2009
Available online 31 October 2009

Keywords:
Coatings
Gold
Raman scattering
Surface structure
Electrospinning
Fractal

ABSTRACT

The ultrafine polymethylmethacrylate fibers containing gold nanoparticles have been prepared by using the electrospinning technique. Then the continuously coarse gold films formed by fractal-like thorny gold particles were deposited on the organic eletrospun fiber surface by an electroless process. The morphology of coarse gold films was characterized by scanning electron and transmission electron microscopy. The results revealed that the morphology of the gold particles was affected not only by the amount of gold seeds embedded in the organic fibers but also by the amount of gold deposited on the fiber's surfaces. The surface-enhanced Raman scattering (SERS) effect of the fibrous mats coated with gold films was evaluated by using Rhodamine B as an adsorbate. The results indicated that this kind of fibrous mat exhibited high and reproducible SERS activity and could be developed as highly sensitive SERS substrate.

1. Introduction

Nano-structured metal materials with controlled shape have attracted a great deal of attention because their optical, electronic and magnetic properties are strongly dependent on the sizes and shapes [1–3], so nano-scaled particles with such shapes as nanorods, nanowires, nanoplates and nanocubes [4–11] have been synthesized in order to investigate their properties. Recently, it has been shown that AgCl is a useful morphological adjusting reagent for the fabrication of the thorny gold particles in aqueous medium [12,13]. Up to the present, nano-structured metal materials have been proven to be the convenient surface-enhanced Raman scattering (SERS) substrates for the vibrational information of the adsorbate [14], and many such materials as assembly-films of silver particles, three-dimensional gold particles, silver surface modified with gold and gold–silver bimetallic particles have been synthesized and used as SERS substrate on which the vibrational signals of the adsorbate have been observed even at a very low concentration [15–18]. It has been shown that SERS depends strongly on the properties of the metallic surface, especially on the morphology and the surface plasmon resonance frequency. Generally, a rough surface can be essentially described as fractal object with self-similitude at different dimension scales [19]. The high efficiency of the near-field enhancement such as SERS has been observed on the rough surfaces with different fractal geometries [20] including the surfaces of the electrode [18] and the nanoparticles [16].

On the other hand, the fibrous mats fabricated by electrospinning technique have stimulated much interest in the past decade due to their large surface-area-to-volume ratio and the potential applications in tissue engineering, sensor, catalysis and so on [21,22]. Nowadays, many hybrid fibrous materials containing inorganic and organic components have been fabricated by the electrospinning technique [23–25]. Moreover, the metallic fibers or micro-tubes have also been fabricated by using the nonwoven eletrospun fibers as templates [26–29]. Furthermore, the electrospinning derived-carbon fibrous mats and the gold-coated eletrospun polyacrylonitrile fibrous mats have been prepared and used as high-quality electrodes [30,31]. However, the electrospun fibrous mats coated with the irregular thorny gold particles have not been fabricated yet.

In this paper, the polymethylmethacrylate (PMMA) fibers containing different amounts of gold nanoparticles (GNPs) are prepared by using an electrospinning method firstly, then the GNPs dispersed on the surface of the fibers are used as gold seeds and enlarged by electroless process during which the morphology of the grown GNPs is influenced by the additional $AgNO_3$ in the plating solution. The morphology changes of the gold particles have been illuminated, and the SERS activity of these fibrous mats coated with irregular thorny gold particles has also been investigated by using Rhodamine B (RhB) as an adsorbate.

* Corresponding author. Tel.: +86 351 7010699; fax: +86 351 7016358.
E-mail address: han_gaoyis@sxu.edu.cn (G. Han).

0040-6090/$ – see front matter © 2009 Elsevier B.V. All rights reserved.
doi:10.1016/j.tsf.2009.10.148

2. Experimental details

2.1. Materials

The reagents such as RhB, tetrabutylammonium bromide (TBAB), silver nitrate ($AgNO_3$), hydrogen tetrachloroaurate ($HAuCl_4 \cdot 3H_2O$) and hydroxylamine hydrochloride ($NH_2OH \cdot HCl$), methylmethacrylate (MMA), potassium persulfate ($K_2S_2O_8$) and cetyltrimethylammonium bromide (CTAB) were analytical grade and obtained from Beijing Chemicals Company and used without further purification. The organic gold salt was synthesized through reacting $HAuCl_4 \cdot 3H_2O$ with TBAB [26]. The plating solutions were prepared by using double-distilled water. The PMMA powders were synthesized as in the following by consulting the previous method [32]: in order to remove the inhibitor, the reagent-grade MMA was firstly washed by 5% NaOH aqueous solution, and then washed by water adequately, thereafter it was distilled under decompression after being dried. After the MMA monomer (5.5 g) was added into the 100 ml aqueous solution of CTAB (5%), the mixture was purged for 40 min with Ar to remove the dissolved oxygen and then heated to about 60 °C at Ar atmosphere under stirring. Then the polymerization was initiated by injecting 1 ml aqueous solution containing 5.5 mg $K_2S_2O_8$. After the mixture was stirred overnight, methanol was added into the mixture to precipitate the product which was collected and washed by water to remove the surfactant completely and dried under vacuum at 50 °C.

2.2. Preparation of the PMMA fibrous mats coated with irregular thorny gold particles

The electrospinning solution was prepared by dissolving the PMMA powder (20 mg) and gold salt (6.0 or 12.0 mg) into 1.0 ml chloroform in which 50 μl DMF was contained. The electrospinning process was carried out at a potential of +8.0 kV after the solution was transferred into a plastic pipette with a nozzle of about 0.5 mm in which a thin platinum rod was connected with the high potential power supply. The electrospun fibers were collected on a filter paper placed upon an electrically grounded aluminum foil 12 cm below the nozzle tip. The hybrid fibrous mats of PMMA/gold salt were defined as 6S and 12S for the samples prepared from the electrospinning solution containing 6.0 and 12.0 mg gold salt, respectively. Prior to the preparation of the gold coating, all glassware was soaked in aqua regia for 1 h, and then thoroughly cleaned with distilled water. After drying for 10 h at room temperature, the fibrous mat together with filter paper was cut into a round shape with a diameter of 4.0 cm, and then placed into a vacuum funnel. Subsequently, the dilute $NaBH_4$ solution (10 mmol L^{-1}, 200 ml) was filtered through the mat in order to reduce the gold salt in the fibers and to form the GNPs embedded in PMMA fibers. Thereafter, the mat was washed with 400 ml 0.1 mol L^{-1} HCl solution and 600 ml water by filtrating, respectively. Finally, the gold nanoparticles immobilized on polymer surface as seeds were enlarged through filtrating 200 ml or 400 ml plating solution until the filtrate became colorless. The typically electroless plating solution used in this paper contained 2.5×10^{-4} mol L^{-1} $HAuCl_4 \cdot 3H_2O$ and 8.0×10^{-4} mol L^{-1} $NH_2OH \cdot HCl$ in which a little amount of $AgNO_3$ was added (1.25×10^{-6} mol L^{-1}) in order to adjust the morphology of the gold particles. The properties of the samples and the conditions of preparation were summarized in the Table 1. At the same time, the thorny gold particles were also prepared in solution according to the previous method [12] at the same $AgNO_3$ concentration.

2.3. Characterization of the thorny gold-coated fibrous mats

UV–visible spectra of the fractal-like gold particles were carried out on a Hewlett Packard 8453E single beam diode array recording spectrophotometer after the thorny gold particles coated on the fibers were dispersed in the chloroform under ultrasonic condition. A piece of the gold-coated mats was placed on the films accessory, and its X-ray diffraction (XRD) pattern was recorded on a Bruker D8 Advance X-ray diffractometer with Cu Kα radiation and graphite monochromator, at the scan speed of 5°/min with a step size of 0.02°. Scanning electron micrographs (SEM) were taken by using a JEOL-JSM-6700 (Tokyo, Japan) field-emission microscope operated at an accelerating voltage of 15 kV. The transmission electron micrograph (TEM) images were recorded on the H-600-2 transmission electron microscope operated at the accelerating voltage of 75 kV after a tiny piece of hybrid mat peeled from the fibrous mats was placed onto the copper grid containing a little of water and adhered to the grid when the water dried. The fractal dimension of the irregular gold particle-coated fiber surface was determined by fractal box count method based on the SEM images by using the ImageJ program.

2.4. Adsorption of RhB on gold-coated fibrous mats for SERS measurement

For SERS measurements, the irregular thorny gold-coated PMMA fibrous mats (3×3 mm^2) were incubated in 5×10^{-6}–5×10^{-12} mol L^{-1} RhB aqueous solution (10 ml) for 10 h. Subsequently, the substrates were rinsed thoroughly with distilled water, and finally dried in a dark atmosphere at room temperature for the test. The thorny gold particles prepared in solution (6 ml) were concentrated and washed by centrifugation (10,000 rpm, 5 min) procedure. Thereafter, the thorny particles were incubated in 5×10^{-6} mol L^{-1} RhB aqueous solution (10 ml) for 10 h, then the colloids adsorbing RhB were loaded on the clean glass slide and let dry under dark in air for SERS measurement after they were concentrated by centrifugation and washed by water. The Raman spectra of the RhB adsorbed on the substrate were recorded on a Jobin Yvon LabRAM HR800 microscopic confocal Raman spectrometer by employing 514.5, 632.8, and 785 nm laser as incident light, a charge coupled device as detector with a resolution 4 cm^{-1}, and an 10×, 0.75 NA objective for focusing the laser light on the samples. The acquisition time for each measurement was 30 s and the spectra were recorded by accumulating the measurement for three times.

Table 1
The characters of the samples prepared from different condition.

*Samples	Gold salt (mg)	C_{AgNO3} mol L^{-1}	$V_{plating\ solution}$ (ml)	Average diameter of the fibers (nm)	Conductivity S cm^{-1}	Fractal dimension	Unitary intensity (1650 cm^{-1})
6S	6.0	–	–	680	–	–	–
6S1	6.0	1.25×10^{-6}	200	1270	4.7×10^{3}	1.8835	0.81
6S2	6.0	1.25×10^{-6}	400	1870	6.9×10^{3}	1.8136	1.00
12S	12.0	–	–	490	–	–	–
12S1	12.0	1.25×10^{-6}	200	1330	6.8×10^{3}	1.8500	0.62
12S2	12.0	1.25×10^{-6}	400	1730	1.3×10^{4}	1.8382	0.48

*The fibrous mats were prepared from 1.0 ml $HCCl_3$ solution containing 20 mg PMMA.

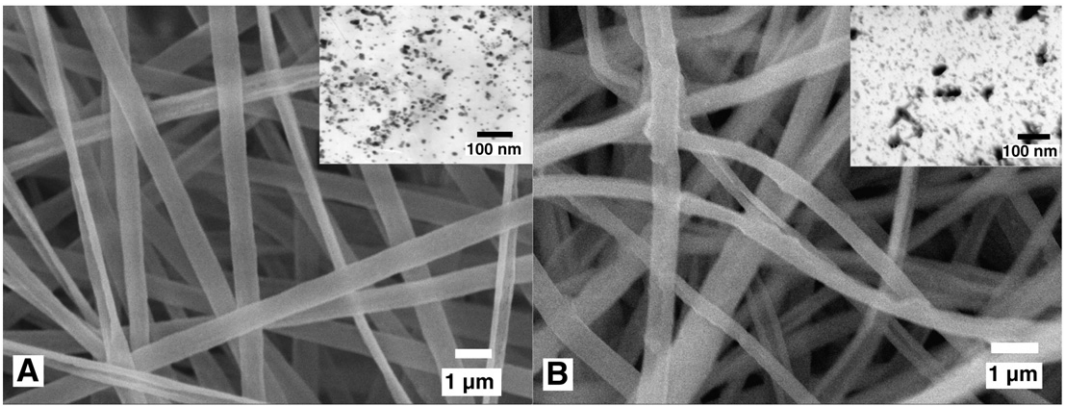

Fig. 1. The microscopical images of the PMMA/GNPs hybrid fibrous mats obtained by treating the PMMA/gold salt fibers with $NaBH_4$ solution (A) from 6S and (B) from 12S, the inserted figures are the TEM images of the corresponding fibers.

3. Results and discussion

3.1. Synthesis and characterization of the fibrous mats coated with irregular thorny gold particles

From the SEM images shown in Fig. 1, we can find that the electrospun PMMA/GNPs hybrid fibers exhibit a random orientation in the fibrous mats due to the bending instability associated with the spinning jet. The average diameter of the fibers is about 680 nm for the PMMA/GNPs fibers prepared from 6S (Fig. 1A), while the diameter of the PMMA/GNPs fibers prepared from 12S decreases to about 490 nm (Fig. 1B) because the electrospinning solution contains more gold salt (12 mg gold salt in 1.0 ml chloroform) which can increase the charge density of the jet and make the fibers thin out during the electrospinning process. The surfaces of the fibers are fairly smooth, which indicates that the GNPs embedded on the fibers' surface are small [33]. The TEM images (inserted figures) show that the amount of the GNPs in PMMA/GNPs fibers prepared from 12S is more than that from 6S, and that the GNPs are roughly spherical in shape and the diameters of most gold particles range from 5 nm to about 30 nm except that some particles aggregate into large clusters.

Fig. 2 shows the SEM images of the PMMA fibers coated with irregular gold particles, from which we can find that the introduced $AgNO_3$ in the plating solution has an important influence on the morphology of the deposited GNPs on the PMMA fibers surface in contrast with the previous report [26] in which the deposited gold particles are almost spherical. We can also find that the organic fibers' surfaces are coated with the continuous gold films assembled by the irregular gold particles, and the average diameter of the fibers in 6S1 is about 1.27 μm (Fig. 2A), the morphology of the gold particles has deviated far from the spherical geometry, while the gold particles with many thorns are observed on the fibers' surface. When the

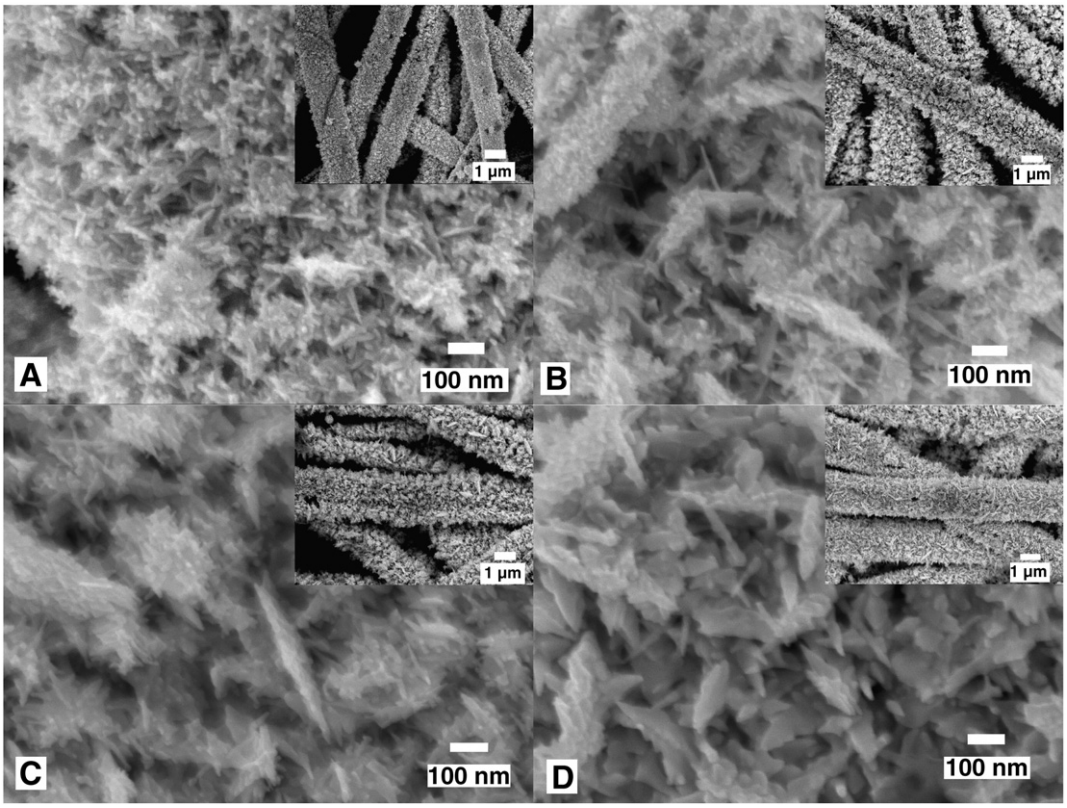

Fig. 2. The SEM images of the fibrous mats coated with irregular gold particles. (A) 6S1, (B) 6S2, (C) 12S1 and (D) 12S2.

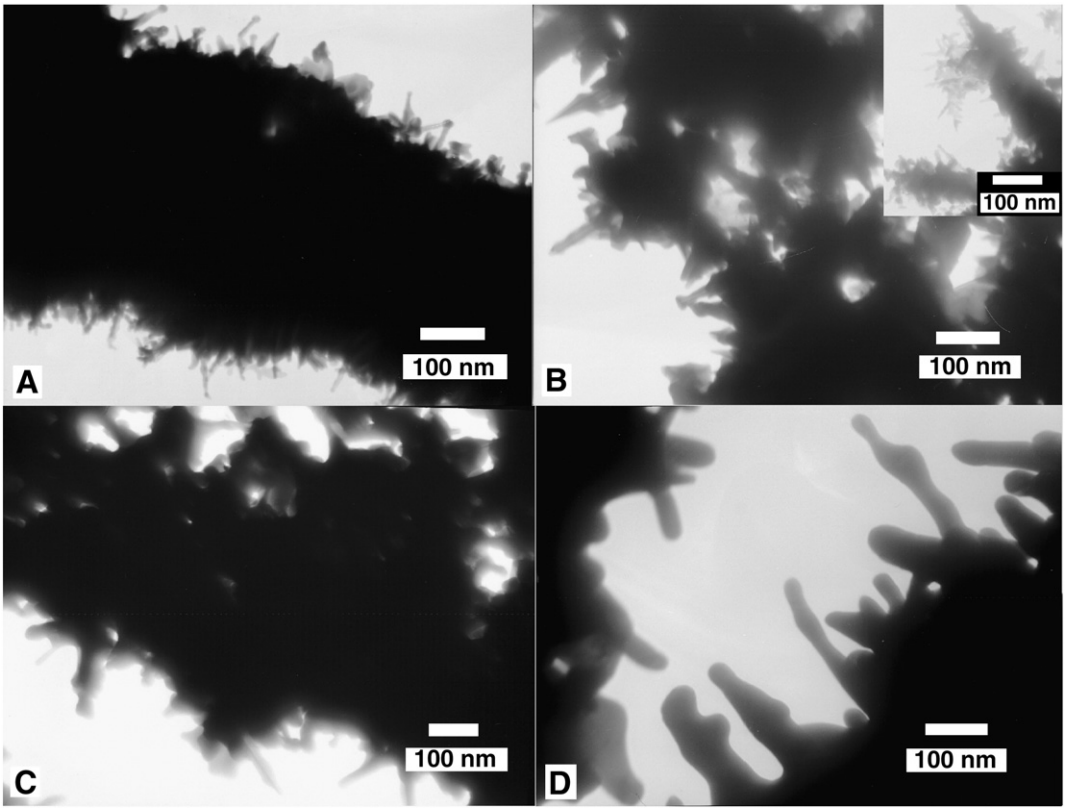

Fig. 3. The TEM images of the fibrous mats coated with irregular gold particles. (A) 6S1, (B) 6S2, (C) 12S1 and (D) 12S2.

samples are prepared by using more plating solution (400 ml), the irregular thorny gold particles together with the gold nano-sheets will be observed on the fibers' surface in 6S2 (Fig. 2B), and the average diameter of the gold-coated fibers increases to about 1.87 μm. When 200 ml plating solution is used to treat the PMMA/GNPs fibrous mats prepared from 12S, the average diameter of the fibers in 12S1 is found to be about 1.33 μm (Fig. 2C), and at the same time the thorny gold particles and the gold sheets are observed on the fibers surfaces. The samples of 12S2 are obtained when 400 ml plating solution is used (Fig. 2D), in which the average diameter of the fibers increases to about 1.73 μm, and the thickness of the gold sheets and thorns increases too.

From the TEM images, we can clearly find that the density of the gold thorns is relatively high in 6S1 (Fig. 3A), and the diameters of the thorns are about 10 nm and the length about 50 nm, while the diameter of the thorns increases to about 20 nm and the length increases to about 100 nm in 6S2 (Fig. 3B). Moreover, some large gold thorns whose diameter at the bottom is larger than 100 nm and length longer than 200 nm (inserted image in Fig. 3B) have also been formed, and there are some small thorny gold particles dispersed on these large gold thorn surfaces. The thorns in 12S1 have a length of about 100 nm and a diameter of about 20 nm (Fig. 3C), while the diameter of the thorns increases to about 20–50 nm, and the length of the thorns can reach to 250 nm in 12S2 (Fig. 3D). From the results mentioned above, we find that the morphology of the fractal-like gold particles deposited on the organic fibers is affected by the amount of the gold seeds in the fibers and the gold deposited on the fibers' surfaces.

In our experiments, the gold particles deposited on the fibers' surface are prepared by filtering the plating solution through the PMMA/GNPs fibrous mats repeatedly, and during which the gold seeds dispersed on the PMMA/GNPs fibers' surface are enlarged through the self-catalyzed reduction of $HAuCl_4$ by NH_2OH. It is shown that the growth process of the gold particles is not continuous in the present condition, which is different from that of the thorny gold particles prepared in solution [12]. During the process of electroless plating, partial surfaces of the gold seeds and the growing gold particles will absorb the formed AgCl which will decrease the growth rate of the gold particles at some direction and lead to the unsymmetrical growth, so the gold particles could not expand isotropically to large gold spheres but form the irregular gold particles. When a small quantity of the plating solution (200 ml) is used to filtrate through the PMMA/GNPs mats containing less gold seeds, the amount of AgCl adsorbed on the gold seeds and growing gold particles is relatively more, which leads to the formation of gold particles with thin thorns in 6S1. When 400 ml plating solution is used to prepare 6S2, the large-sized gold thorns and gold sheets are formed because of the higher amount of AgCl adsorbed on the growing gold particles and the higher amount of the deposited gold. At the same time, the large thorny

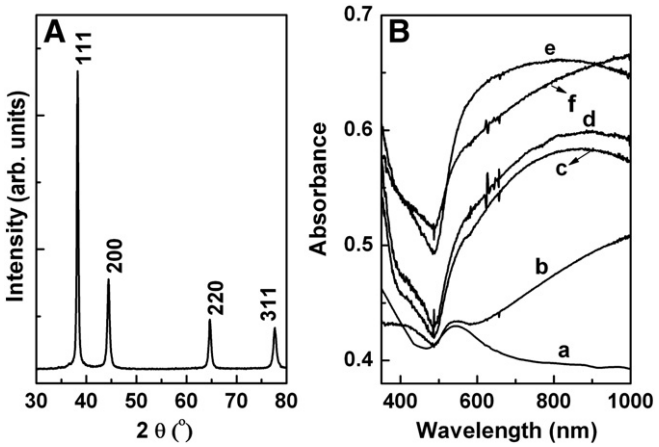

Fig. 4. (A) the XRD pattern of the irregular gold particle-coated fibrous mats 6S2, (B) the SPR absorption spectra of the spherical gold particles (a), thorny gold particles prepared in solution (b), and irregular gold particles in 6S1, 6S2, 12S1 and 12S2 (c)–(f), respectively.

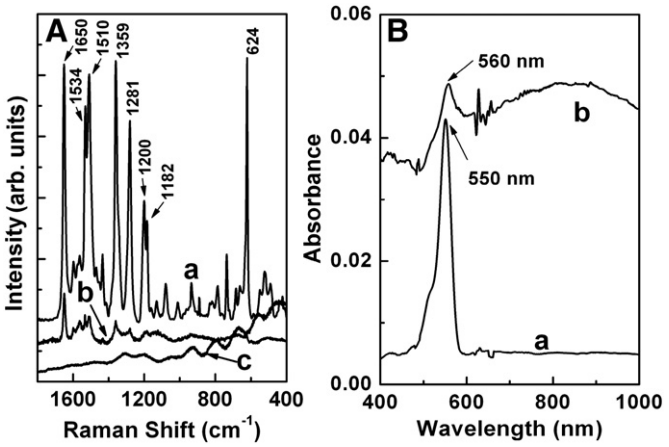

Fig. 5. (A) The SERS spectra of RhB adsorbed on 6S2 substrate excited by different incident light, (a) 632.8, (b) 514.5 and (c) 785 nm laser, and (B) the UV–vis spectra of the RhB (a) and the RhB adsorbed on 6S2 (b) dispersed in chloroform.

surface is coated with many small thorns. This result indicates that the formed AgCl is high enough to coat the large thorny surfaces, so the small thorns are formed on the large thorns surface during the following gold plating process. When the fibrous mat containing more gold seeds is treated with the same amount of plating solution, the number of the gold seeds and the growing gold particles increase much more in this case, so the amount of AgCl adsorbed on the gold particles surface decreases in contrast with the fibers containing less GNPs. Therefore, the irregular thorny gold particles including gold sheets and thorny gold particles are deposited on the fibers surface in 12S1. When more plating solution (400 ml) is used, the thickness of the gold sheets and the size of the gold thorn increase obviously, however, there are not many small thorns observed on the large thorny surface. The result obtained indicates that the amount of gold seeds in the fibers has an important effect on the morphology of the deposited gold particles because they can adjust the relative density of the AgCl absorbed on the gold particles, which is similar to the previous reports [12,17] in which the thorns' thickness decreases with the increase of $AgNO_3$ amount, and increases with the increase of the amount of deposited gold.

The XRD patterns of the fibrous mats coated with irregular gold particles show the typical fcc gold characteristics (PDF 4-784), the peaks at 38.22, 44.43, 64.64, and 77.63° are assigned as (111), (200), (220), and (311) plane reflections of gold (Fig. 4A), respectively. The conductivities of the gold-coated fibrous mats have been measured by using the four-probe method and the conductivities of 6S1, 6S2, 12S1 and 12S2 are found to be about 4.7×10^3, 6.9×10^3, 6.8×10^3 and 1.3×10^4 S cm^{-1}, respectively. The conductivities increase with the increase of the amount of deposited gold and the embedded gold seeds, this is because that more gold seeds in the organic fibers will lead to more gold particles formed on the fibers surface, which may cause the gold particles to contact closely and increase the conductivity.

It is well known that the surface plasmon resonance (SPR) absorptions of metal nanoparticles such as gold and silver are dependent on particle shape, size, and interactions between particles and the dielectric constant of the surrounding medium [34,35]. The deviations from spherical geometry generally cause the SPR absorptions to red shift. From Fig. 4B, we can find clearly that the spectra of the irregular thorny gold particles are completely different from that of spherical gold particles. The spherical GNPs exhibit a SPR peak at about 530 nm (Fig. 4B-a), while the thorny gold particles prepared in solution [12] show a strong SPR absorption at long wavelength region and a weaker SPR peak at 530 nm (Fig. 4B-b). The irregular gold particles in 6S1 show a shoulder SPR peak at about 560 nm and a broad SPR peak at about 850 nm (Fig. 4B-c), while the irregular gold particles in 6S2 show a broad SPR peaks at about 890 nm (Fig. 4B-d) because of the increase of deposited gold quantity. The similar SPR absorptions are also observed for the irregular gold particles in 12S1 and 12S2. For example, the irregular gold particles in 12S1 show a broad and strong SPR absorption peak at about 807 nm (Fig. 4B-e) and particles in 12S2 (Fig. 4B-f) show the SPR absorption peak in longer wavelength region because more gold is deposited in 12S2.

3.2. The SERS property of the fibrous mats coated with the irregular gold particles

Fig. 5A represents the Raman spectra of the RhB adsorbed on the substrate of 6S2 in which the 514.5, 632.8 and 785 nm lasers are used as incident light, respectively. We can find that the intensity of the SERS signal is the strongest when the 632.8 nm laser is used as exciting light, and that only weak SERS signals can be observed at 1600–1200 cm^{-1} when 514.5 nm laser is used as exciting light. However, there are no obvious SERS signals observed if the substrate is excited by 785 nm laser. The strong peaks at about 1650, 1534, 1510 and 1359 cm^{-1} are assigned to the aromatic C—C stretching modes. The bands centered at about 1281, 1200 and 1185 cm^{-1} are assigned to the C—C bridge-bands stretching and in-plane C—H bend of the aromatic ring moiety of the molecule, and the strong band centered at about 624 cm^{-1} is assigned to the aromatic bending [36–39]. The UV–vis spectra show that RhB exhibits a strong absorption peak at 550 nm (Fig. 5B-a) in chloroform, while the absorption spectra of the RhB

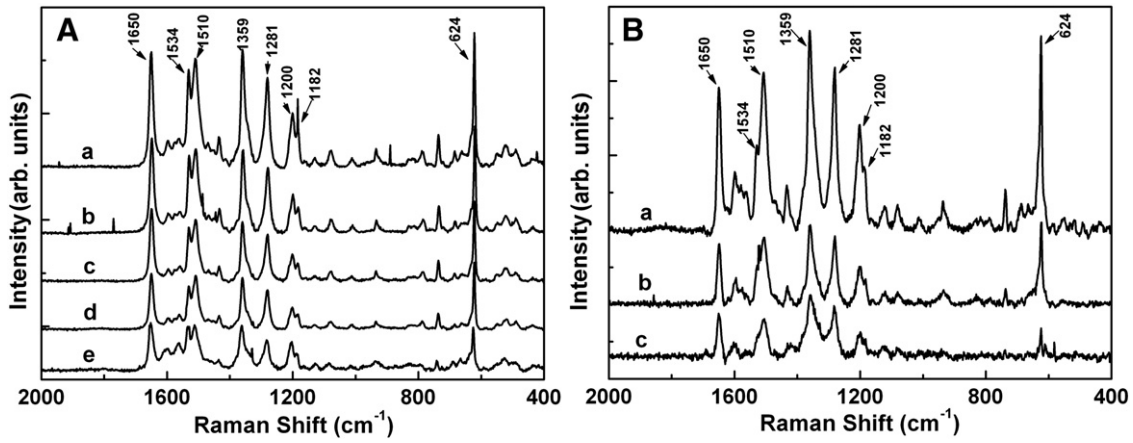

Fig. 6. (A) The SERS spectra of RhB adsorbed on (a) 6S2, (b) 6S1, (c) 12S1, (d) 12S2 and (e) thorny gold particles prepared in solution by using the reported method, the 5×10^{-6} mol L^{-1} RhB solution (10 ml) is used to incubate the substrates. (B) The SERS spectra of RhB adsorbed on 6S2 by using (a) 5×10^{-8}, (b) 5×10^{-10} and (c) 5×10^{-12} mol L^{-1} RhB solution (10 ml) as incubated solution. The wavelength of exciting laser is 633 nm.

adsorbed on 6S2 show the features of RhB and 6S2, an absorption peak at 560 nm together with the SPR absorption of the gold particles in long wavelength region (Fig. 5B-b). From the experiments, we can find that the SERS signal of RhB can only be observed when the wavelength of the exciting laser is near the absorption peak of RhB. It is well known that the SERS phenomenon is often attributed to the electromagnetic (EM) and chemical (CHEM) enhancement. The EM mechanism is based on the amplified electromagnetic field generated upon optical excitation of SPR of the noble metals with a coarse surface in nano-scale [40,41]. The CHEM effect in SERS mainly results from two aspects, one is that the electronic coupling between the adsorbed molecules and the metal surface at atomic-scale roughness will lead to the charge transfer between the adsorbate and metal surface, which increases the polarizability of the molecule and the Raman scattering cross section [42,43], the other is the resonances within the adsorbed molecule itself especially for the highly colored molecules [44]. It is widely accepted that the combination of the EM and CHEM enhancement causes the SERS enhancement [6,44]. According to the experiments and the features of the gold particles, we can conclude that the chemical effects contribute significantly to the enhancement for RhB besides the EM enhancement. Based on the stronger Raman peak of RhB centered at about 1650 cm^{-1}, we find that the SERS intensity of RhB adsorbed on the substrate of 6S2 (Fig. 6A-a) is the strongest, and that on the thorny particles prepared in solution is the lowest (Fig. 6A-e). When the lower concentration such as 5×10^{-8} mol L^{-1} RhB solution is used to incubate the selected optimal SERS substrate 6S2, the SERS signals of RhB can easily be observed except that the peaks at 1534 and 1182 cm^{-1} become weak (Fig. 6B-a). When the concentration of RhB solution decreases to 5×10^{-10} and 5×10^{-12} mol L^{-1}, the SERS intensity of the absorbed RhB decreases with the decrease of the concentration of the incubated RhB solution (Fig. 6B-b,c), but we can still clearly observe the SERS scattering spectra of RhB adsorbed on the optimum substrate 6S2 when the concentration of the incubated RhB solution is as low as 5×10^{-12} mol L^{-1}.

4. Conclusions

In this work, the continuous films assembled by irregular thorny gold particles have been fabricated on the ultrathin electrospun PMMA fibers surface. The results show that the morphology of the irregular thorny gold particles is affected not only by the amount of gold seeds but also by the amount of gold deposited on the fibers' surface. The SERS intensity of RhB adsorbed on the fractal-like gold-coated fibrous mats is stronger than that on the thorny gold particles prepared in solution. Moreover, obvious SERS signals of RhB can be observed on the optimum thorny gold-coated fibrous mats although the incubated solution concentration is as low as 5×10^{-12} mol L^{-1} (10 ml). The irregular gold particle-coated PMMA fibrous mats may be developed as a new, convenient and highly sensitive SERS substrate.

Acknowledgments

The authors thank the National Natural Science Foundation of China (No. 20604014), Shanxi province (No. 2007021008), and the Program for the Top Young and Middle-aged Innovative Talents of Higher Learning Institutions of Shanxi (TYMIT and TYAL) and the foundation of Shanxi University.

References

[1] C. Burda, X. Chen, R. Narayanan, M.A. El-Sayed, Chem. Rev. 105 (2005) 1025.
[2] C.J. Murphy, T.K. Sau, A.M. Gole, C.J. Orendorff, J. Gao, L. Gou, S.E. Hunyadi, T.J. Li, J. Phys. Chem. B 109 (2005) 13857.
[3] L.M. Liz-Marzan, Langmuir 22 (2006) 32.
[4] F. Kim, J.H. Song, P.D. Yang, J. Am. Chem. Soc. 124 (2002) 14316.
[5] N.R. Jana, L. Gearheart, C.J. Murphy, Adv. Mater. 13 (2001) 1389.
[6] J.T. Zhang, X.L. Li, X.M. Sun, Y.D. Li, J. Phys. Chem. B 109 (2005) 12544.
[7] K. Vasilev, T. Zhu, M. Wilms, G. Gillies, I. Lieberwirth, S. Mittler, W. Knoll, M. Kreiter, Langmuir 21 (2005) 12399.
[8] C.S. Ah, Y.J. Yun, H.J. Park, W. Kim, D. Ha, W.S. Yun, Chem. Mater. 17 (2005) 5558.
[9] M. Yamamoto, Y. Kashiwagi, T. Sakata, H. Mori, M. Nakamoto, Chem. Mater. 17 (2005) 5391.
[10] S.H. Im, Y.T. Lee, B. Wiley, Y.N. Xia, Angew. Chem. Int. Ed. 44 (2005) 2154.
[11] D.B. Yu, V.W. Yam, J. Am. Chem. Soc. 126 (2004) 13200.
[12] H. Yuan, W.H. Ma, C.C. Chen, J.C. Zhao, J.W. Liu, H.Y. Zhu, X.P. Gao, Chem. Mater. 19 (2007) 1592.
[13] C.L. Nehl, H.W. Liao, J.H. Hafner, Nano Lett. 6 (2006) 683.
[14] P.A. Mosier-Boss, S.H. Lieberman, Langmuir 19 (2003) 6826.
[15] Y. Lu, G.L. Liu, L.P. Lee, Nano Lett. 5 (2005) 5.
[16] G.W. Lu, C. Li, G.Q. Shi, Chem. Mater. 19 (2007) 3433.
[17] X.Q. Zou, E.B. Ying, S.J. Dong, J. Colloid Interface Sci. 306 (2007) 307.
[18] Y.C. Liu, C.C. Yu, T.C. Hsu, Electrochem. Commun. 9 (2007) 639.
[19] M. Micic, N. Klymyshyn, H.P. Lu, J. Phys. Chem. B 108 (2004) 2939.
[20] S.I. Bozhevolnyi, B. Vohnsen, A.V. Zayats, I.I. Smolyaninov, Surf. Sci. 356 (1996) 268.
[21] A. Greiner, J.H. Wendorff, Angew. Chem. Int. Ed. 46 (2007) 5670.
[22] D. Li, Y.N. Xia, Adv. Mater. 16 (2004) 1751.
[23] C.H. Sui, R. Yang, R. Yina, J. Gong, C.L. Shao, L.Y. Qu, Thin Solid Films 516 (2008) 3899.
[24] J.S. Jeong, J.S. Moon, S.Y. Jeon, J.H. Park, P.S. Alegaonkar, J.B. Yoo, Thin Solid Films 515 (2007) 5136.
[25] S. Samitsu, T. Shimomura, K. Ito, Thin Solid Films 516 (2008) 2478.
[26] G.Y. Han, B. Guo, L.W. Zhang, B.S. Yang, Adv. Mater. 18 (2006) 1709.
[27] V.G. Pol, E. Koren, A. Zaban, Chem. Mater. 20 (2008) 3055.
[28] M. Bognitzki, M. Becker, M. Graeser, W. Massa, J.H. Wendorff, A. Schaper, D. Weber, A. Beyer, A. Goelzhaeuser, Adv. Mater. 18 (2006) 2384.
[29] F. Ochanda, W.E. Jones, Langmuir 23 (2007) 795.
[30] M.Y. Li, G.Y. Han, B.S. Yang, Electrochem. Commun. 10 (2008) 880.
[31] B. Guo, S.Z. Zhao, G.Y. Han, L.W. Zhang, Electrochim. Acta 53 (2008) 5174.
[32] F. Bleger, A.K. Murthy, F. Pla, E.W. Kaler, Macromolecules 27 (1994) 2559.
[33] G.M. Kim, A. Wutzler, H.J. Radusch, G.H. Michler, P. Simon, R.A. Sperling, W.J. Parak, Chem. Mater. 17 (2005) 4949.
[34] K.L. Kelly, E. Coronado, L.L. Zhao, G.C. Schatz, J. Phys. Chem. B 107 (2003) 668.
[35] S. Link, M.A. El-Sayed, Annu. Rev. Phys. Chem. 54 (2003) 331.
[36] Y.H. He, J.Y. Yuan, G.Q. Shi, J. Mater. Chem. 15 (2005) 859.
[37] J. Sarkar, J. Chowdhury, P. Pal, G.B. Talapatra, Vib. Spectrosc. 41 (2006) 90.
[38] W.C. Ye, C.M Shen, J.F. Tian, C.M. Wang, L.H. Bao, H.J. Gao, Electrochem. Commun. 10 (2008) 625.
[39] P. Hildebrandt, M. Stockburger, J. Phys. Chem. 88 (1984) 5935.
[40] K.L. Kim, S.J. Lee, K. Kim, J. Phys. Chem. B 108 (2004) 9216.
[41] V.S. Tiwari, T. Oleg, G.K. Darbha, W. Hardy, J.P. Singh, P.C. Ray, Chem. Phys. Lett. 446 (2007) 77.
[42] A. Otto, I. Mrozek, C. Pettenkofer, Surf. Sci. 238 (1990) 192.
[43] W.E. Doering, S.M. Nie, J. Phys. Chem. B 106 (2002) 311.
[44] J.R. Lombardi, R.L. Birke, Acc. Chem. Res. 42 (2009) 734.